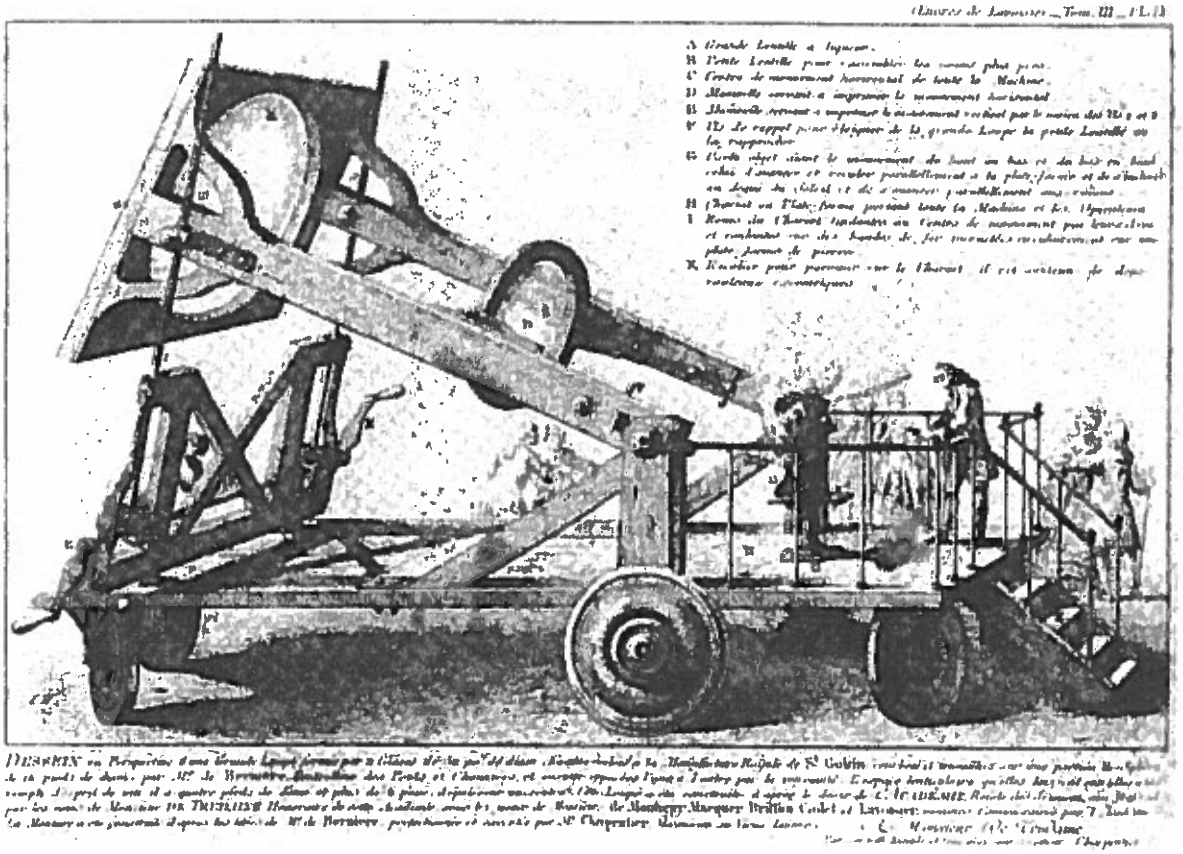

Figure 8.1. Solar furnace used by Lavoisier in 1774. Illustration courtesy of Bibliotheque Nationale de Paris. Lavoisier, *Oeuvres*, vol. 3.

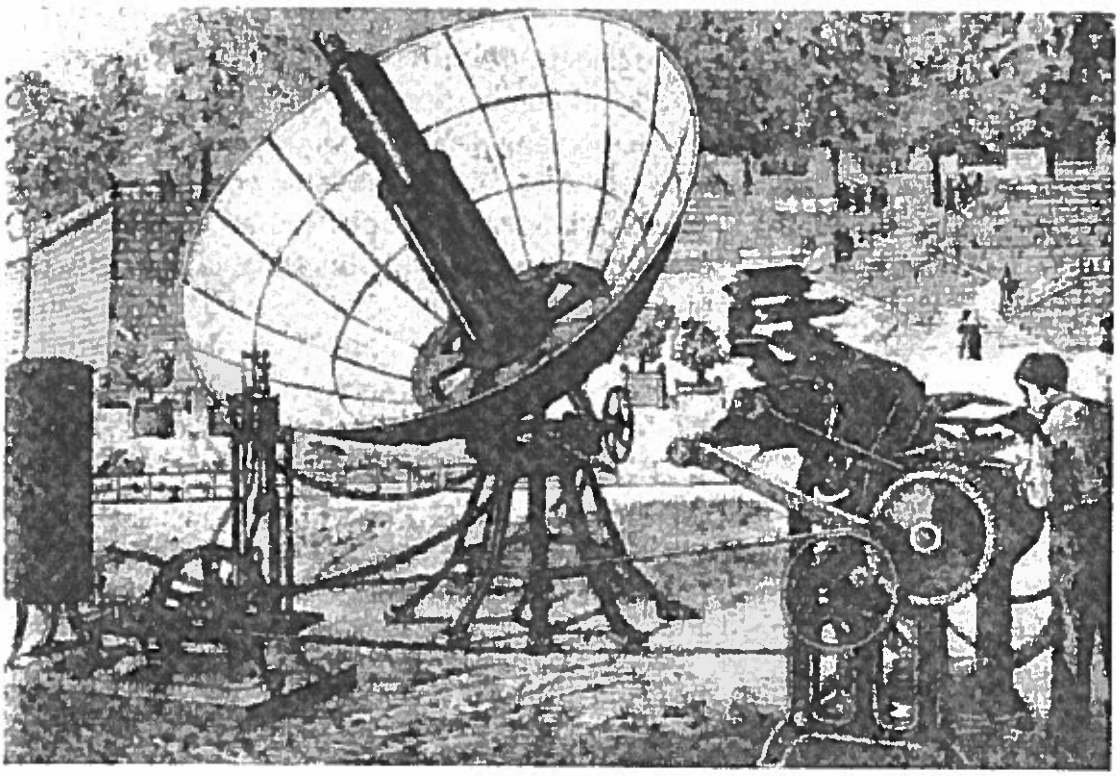

Figure 8.2. Parabolic collector powered a printing press at the 1878 Paris Exposition.

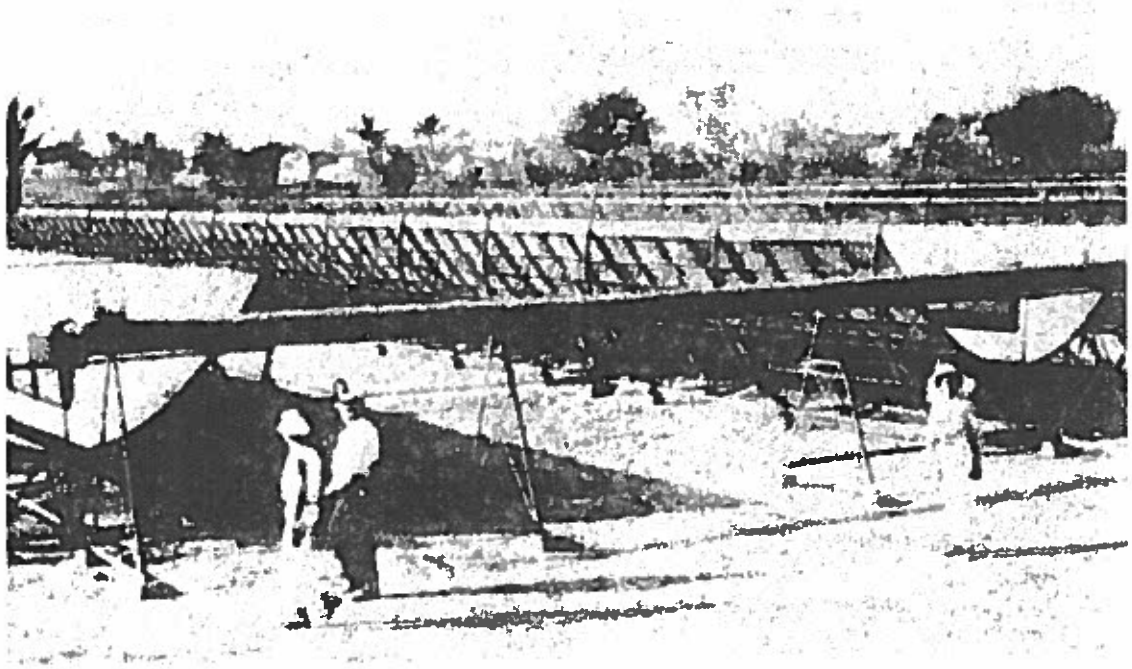

Figure 8.4. Solar irrigation pump (50-hp) operating in 1913 in Egypt.

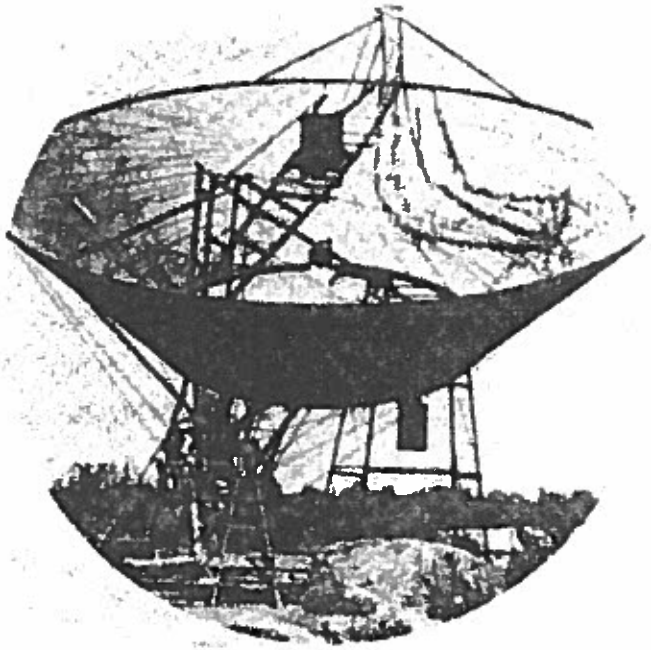

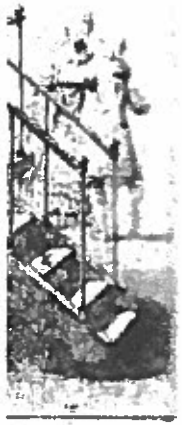

Figure 8.3. Irrigation pumps were run by a solar-powered steam engine in Arizona in the early 1900s. The system consisted of an inverted cone that focused rays of the sun on the boiler.

With the increasing availability of low-cost oil and natural gas, interest in solar energy for power production waned. Except for C.G. Abbott, who exhibited in 1936 a -hp solar-powered engine at an International Power Conference in Washington, D.C. and in 1938 in Florida, an improved, somewhat smaller version with a flash boiler, there was very little activity in the field of solar power between 1915 and 1950. Interest in solar power revived in 1949 when, at the centennial meeting of the American Association for the Advancement of Science in Washington, D.C., one session was de-

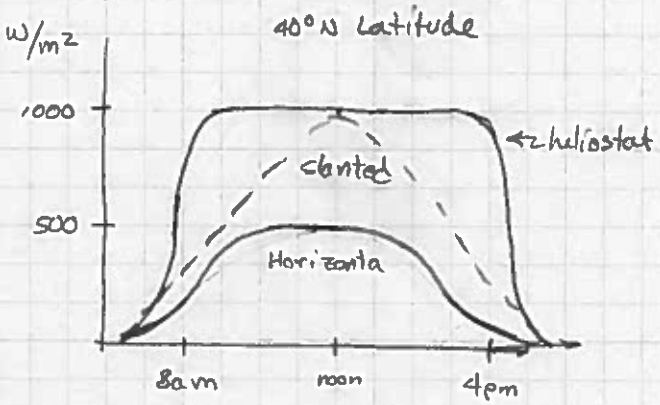

Energy Balance (Flat Plate Collector)

$$I_c \cdot A_c \cdot \tau_s \cdot \alpha_s = \frac{dE_c}{dt} + \Delta \dot{E}_{fluid}$$

- $\frac{dE_c}{dt}$ ← rate of sensible heat accumulation/loss in collector
- α_s ← absorbance at collector-absorber interface
- τ_s ← effective solar transmittance of the collector covers
- I_c ← solar insolation

$$\Delta \dot{E}_{fluid} = \dot{m} C_p \Delta T$$

$$\eta_c = \frac{\Delta \dot{E}_{fluid}}{I_c A_c} \equiv \frac{\text{rate of useful energy delivered}}{\text{total incident solar energy}}$$

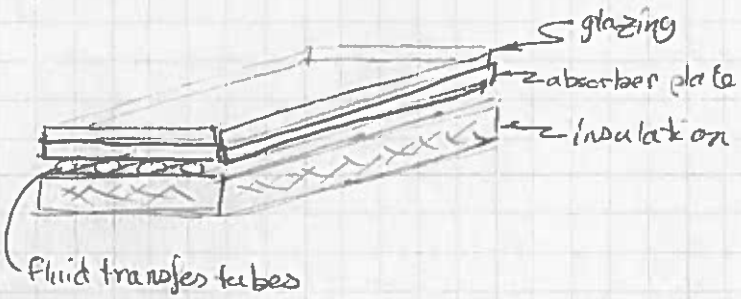

Flat Plate Collectors
- liquid-type
- air-type

- glazing:
  - transmits shorter wavelength solar radiation, but blocks longer wavelength from absorber
  - reduces convective heat transfer losses
  - most common material is glass

Tubular Collectors (Fig 3.17, Gk&k)

- Evacuated-Tube Collectors
  - minimize q_{loss}
  - proposed in 1909; 2 concepts still sold today
  - internal reflectivity serves as pseudo-concentrator

Concentrators

optical concentration ratio, $CR_o = \frac{I_r}{I_a} = \frac{\text{solar flux received}}{\text{solar flux at aperture}}$ } accounts for optical losses

geometric concentration ratio, $CR_A = \frac{A_a}{A_r}$

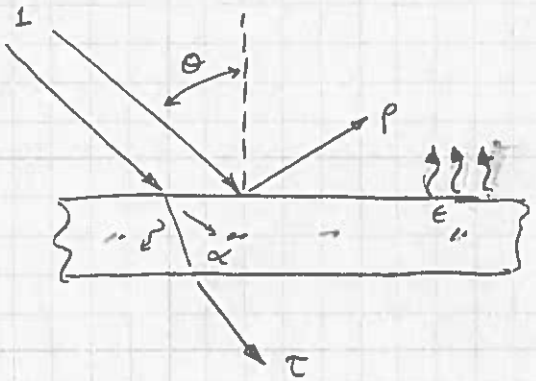

$\rho \equiv$ reflectance

$\tau \equiv$ transmittance

$\alpha \equiv$ absorptance

$\epsilon \equiv$ emittance

} all $f(\theta, \lambda)$

↑ ratio of radiative emission to that of a black body (ideal "black" surface)

ρ can be specular or diffuse

$$\tau + \rho + \alpha = 1$$

monochromatic, directional emittance

$$\epsilon_\lambda(\theta, \phi) = \frac{I_\lambda(\theta, \phi)}{I_{b,\lambda}}$$

$\phi \equiv$ azimuthal angle

$\theta \equiv$ polar angle

$$\epsilon = \frac{1}{\sigma T^4} \int_0^\infty \epsilon_\lambda E_{b_\lambda} \, d\lambda$$

↑ surface properties

monochromatic, directional absorptance

$$\alpha_\lambda(\theta, \phi) = \frac{I_{\lambda,a}(\theta, \phi)}{I_{\lambda,i}(\theta, \phi)}$$

$a \equiv$ absorbed radiation

$i \equiv$ incident radiation

$$\alpha(\theta, \phi) = \frac{1}{I_i(\theta, \phi)} \int_0^\infty \alpha_\lambda(\theta, \phi) I_{\lambda,i}(\theta, \phi) \, d\lambda$$

↑ not just a surface property

- can design selective ~~surfaces~~ materials which absorb radiation from one source at a greater rate than from another source

Tubular Collectors

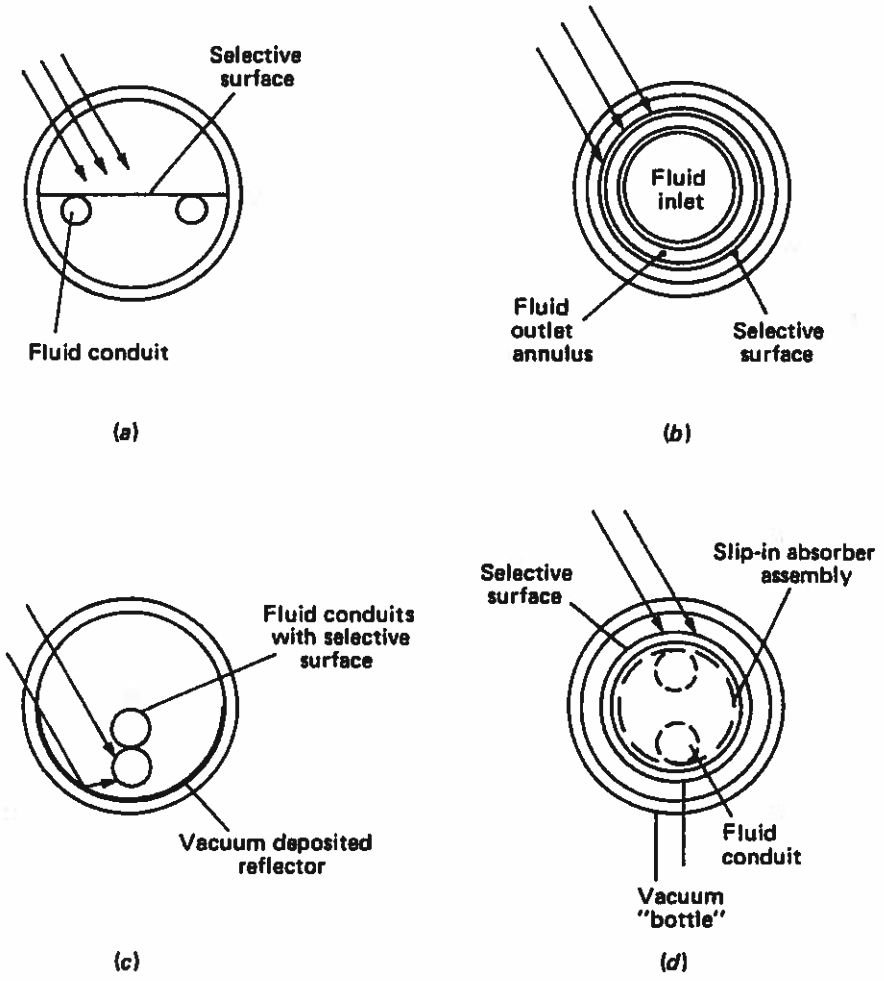

Figure 3.17. Evacuated-tube solar energy collectors: (a) flat plate; (b) concentric tubular; (c) concentrating; (d) vacuum bottle with slip-in heat exchanger contacting rear surface of receiver.

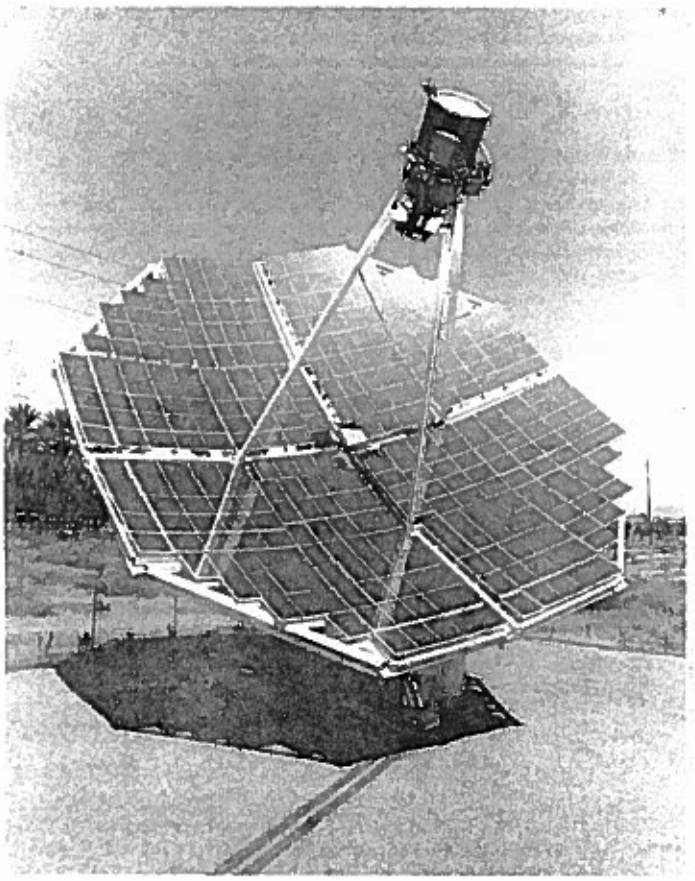

(a)

Figure 3.38. Examples of commercially developed multifaceted and stretched membrane paraboloidal concentrators: (a) multifaceted mirror.

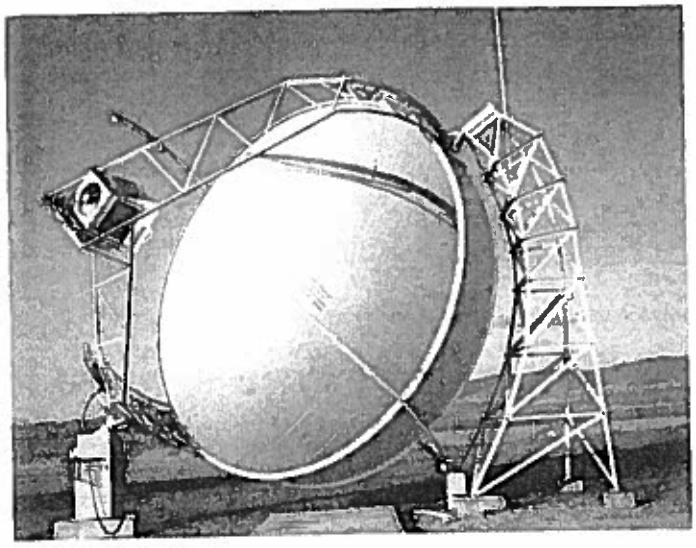

(b)

Figure 3.38. (*continued*) (b) Stretched single membrane (Schlaich Bergermann & Partner [Germany]).

optical concentration ratio,

$$CR_o \equiv \frac{\text{solar flux received}}{\text{aperture solar flux}} = \frac{I_r}{I_a}$$

geometric concentration ratio,

$$CR \equiv \frac{A_{concentrator}}{A_{absorber}}$$

CR_o gives true concentration because it accounts for the optical losses due to reflection & refraction.

CR_o unrelated to receiver area & thus provides no information on thermal losses which are proportional to area.

$$Q_u = \eta_o I_c A_a - U_c (T_c - T_a) A_r$$

(U_c: heat loss conductance)

η_o: optical efficiency $\equiv \frac{\text{solar radiation}}{\text{beam solar}}$ by metric solar

$$\eta_c = \frac{Q_u}{I_c A_a} = \eta_o - \frac{U_c (T_c - T_a)}{I_c} \frac{1}{CR}$$

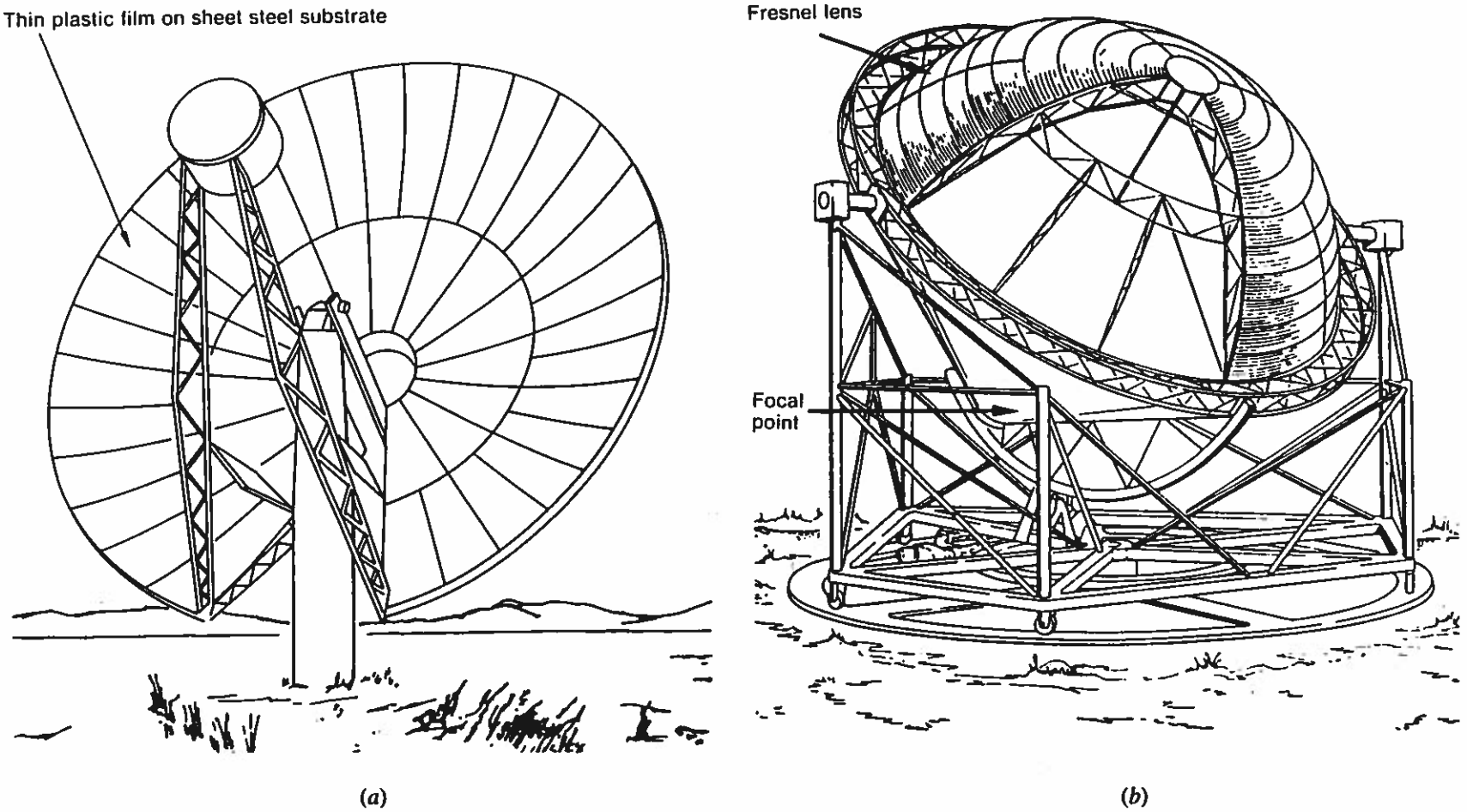

Figure 13-19 Point-focus distributed-type concentrators: (*a*) thin plastic film reflecting panels by Boeing, Inc. (*b*) Fresnel-lens concept by E-Systems Corporation [125].

SOLAR THERMAL ELECTRIC: DISH STIRLING ENGINE

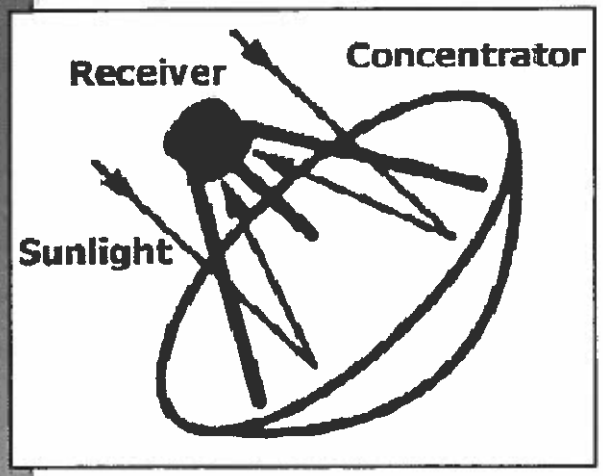

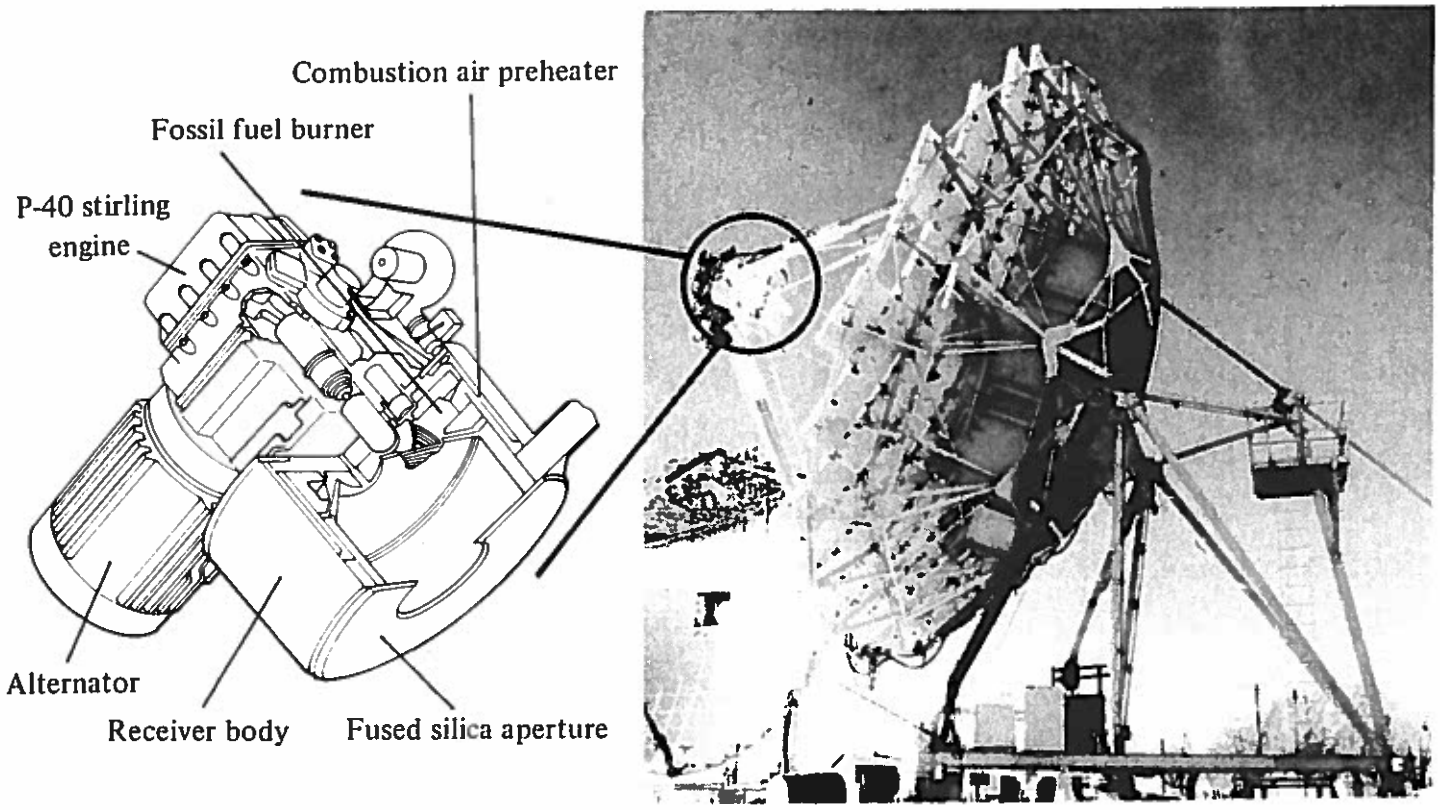

Figure 13-24 JPL test bed with parabolic bed concentrator and Stirling engine. *(Courtesy Jet Propulsion Laboratory.)*

Combined-Cycle Systems

Combined cycles are those using a combination of Brayton- and Rankine-cycle-type powerplants with the gas turbine of the Brayton cycle occupying the high-temperature end and exhausting to the steam generator of the Rankine cycle (Sec. 8-8).

Figure 13-25 shows a combined-cycle with a two-shaft gas turbine and a solar central-receiver system. Atmospheric air is compressed by the compressor into a high-temperature receiver where it is heated to perhaps 1500°F (815°C). It then expands through the compressor turbine and through the power turbine, which drives an electric

SOLAR THERMAL ELECTRIC: PARABOLIC TROUGH

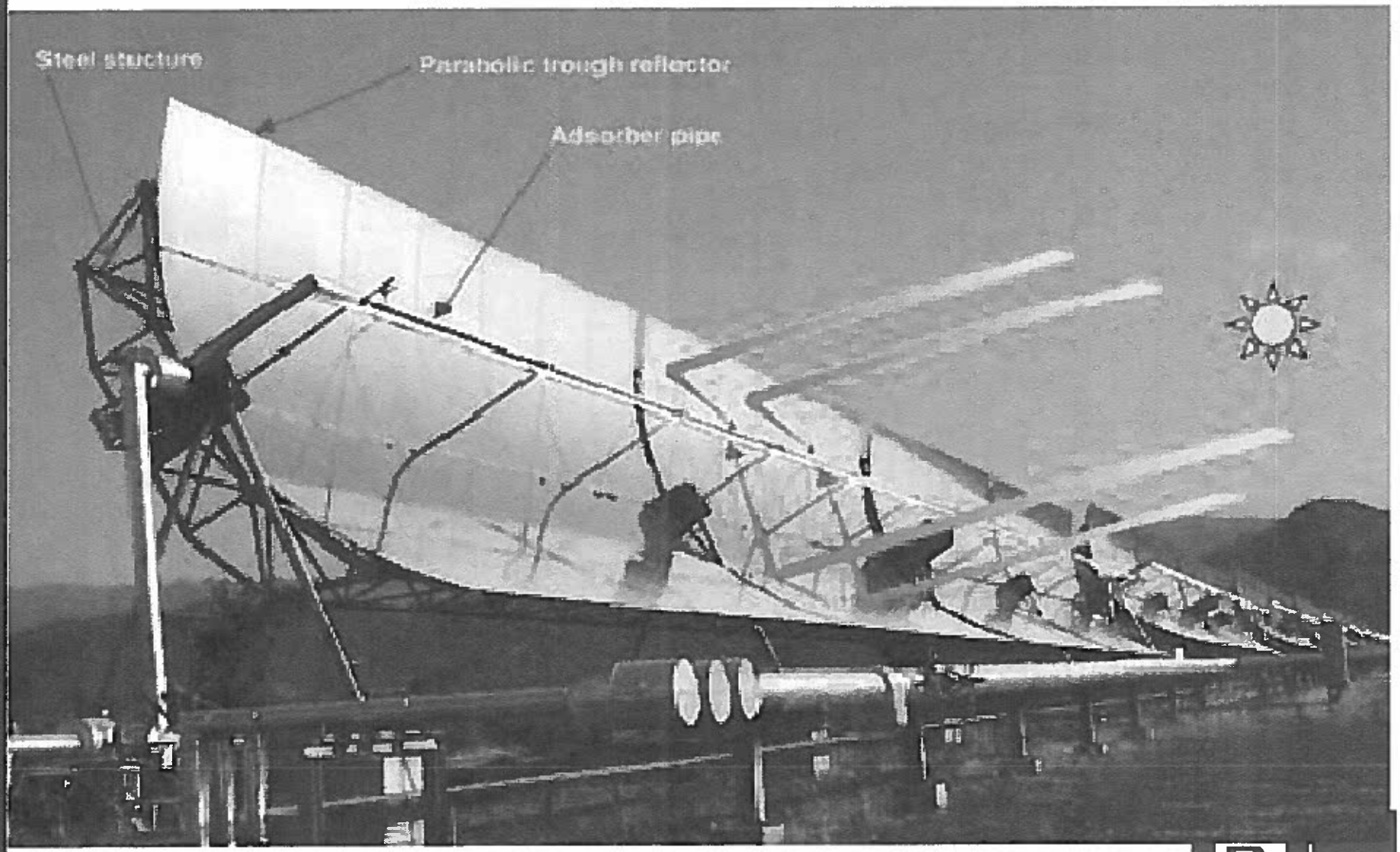

TYPES OF SOLAR ENERGY POWER PLANTS

Parabolic Trough Solar Field

Solar Collection Assemblies

As the Earth rotates, the solar collectors need to be adjusted to optimize the angle of the sun to the collection surface. The mirrors are adjusted about once every minute.

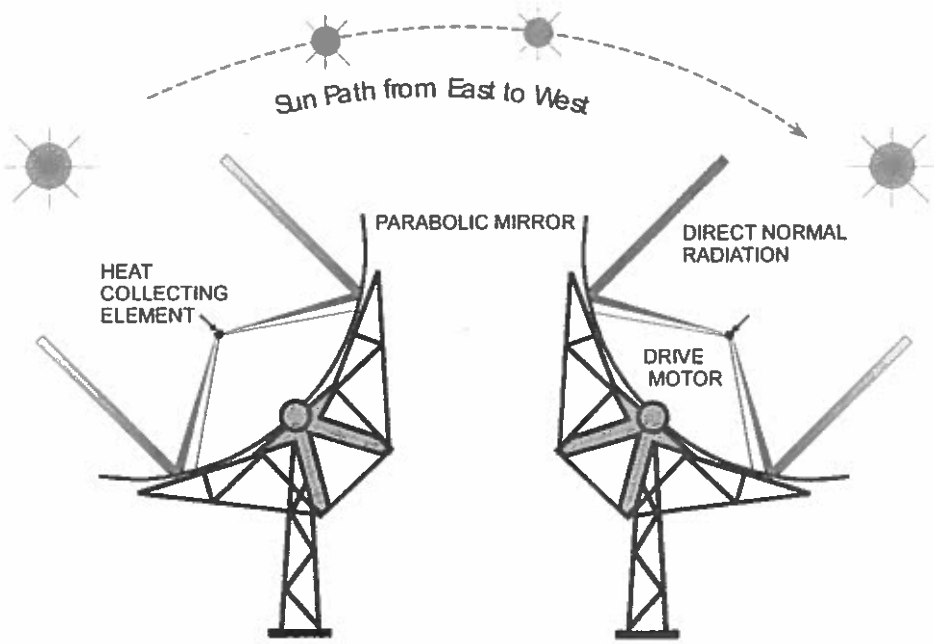

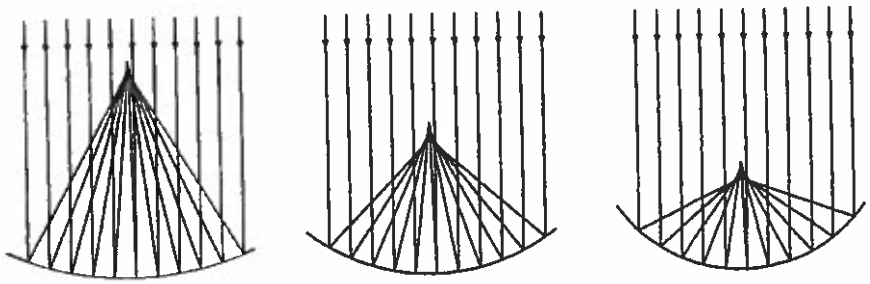

Figure 3.25. Focusing of parallel rays of light using circular mirrors with different rim angles.

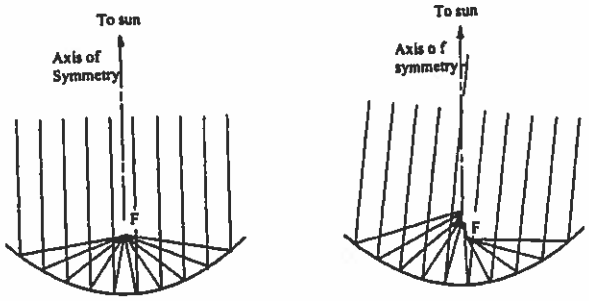

Figure 3.26. Concentration by parabolic reflector for a beam (a) parallel to the axis of symmetry, and (b) at an angle to the axis.

compound parabolic concentrator (CPC)
non-imaging concentrator

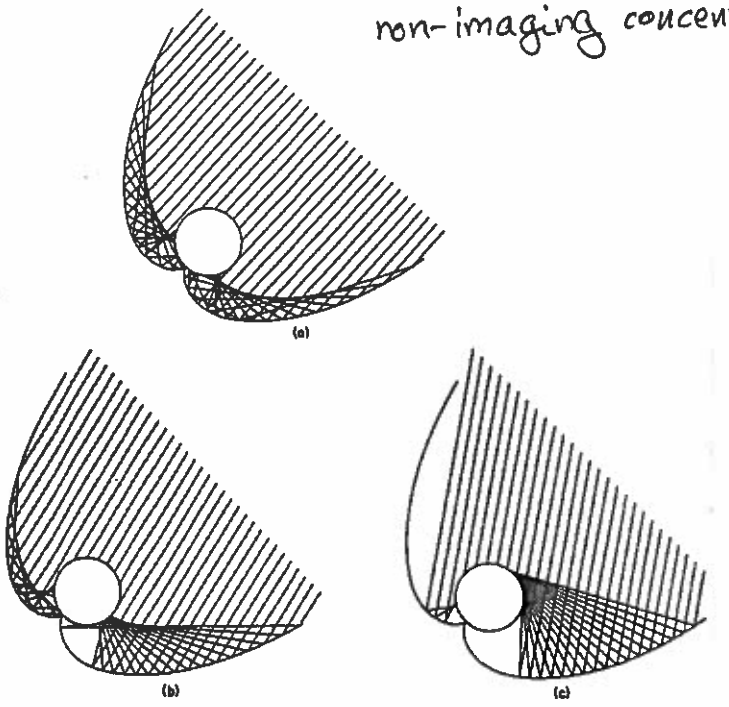

Figure 3.43. Ray trace diagrams of the tubular CPC collector at three values of incidence angle: (a) normal incidence; (b) intermediate; and (c) the limit of acceptance. (Courtesy of W. McIntire, Argonne National Laboratory.)

- fewer optical losses

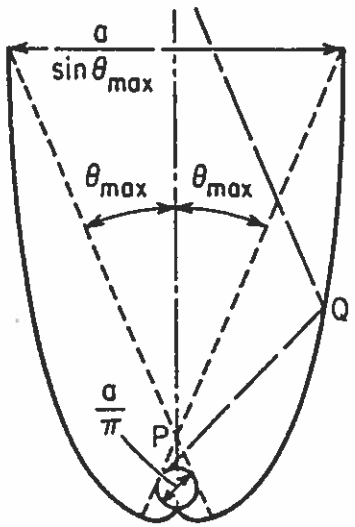

Early Argonne Design

External reflector CPC coupled to evacuated dewar-type absorber with spectrally selective coating

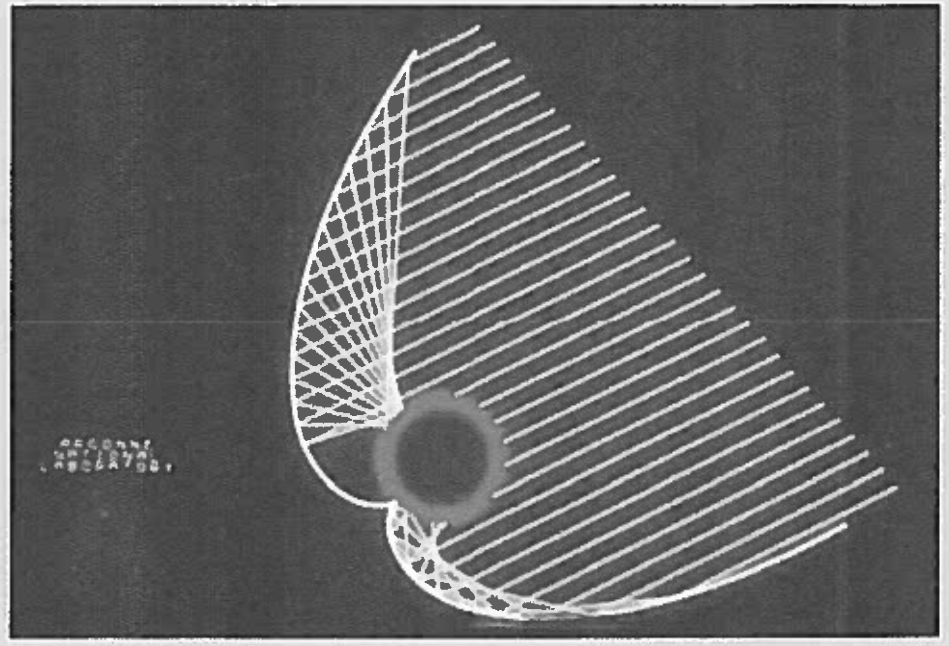

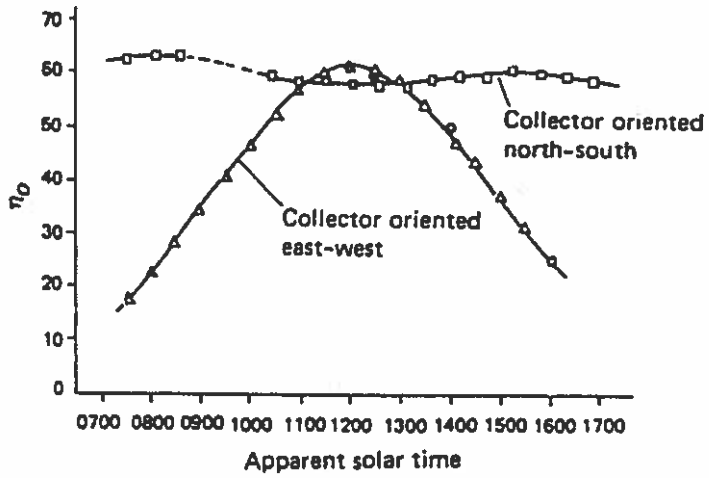

Figure 3.36. Measured optical efficiency of a PTC in north-south and east-west orientations [65]. Adapted from Kreider [43].

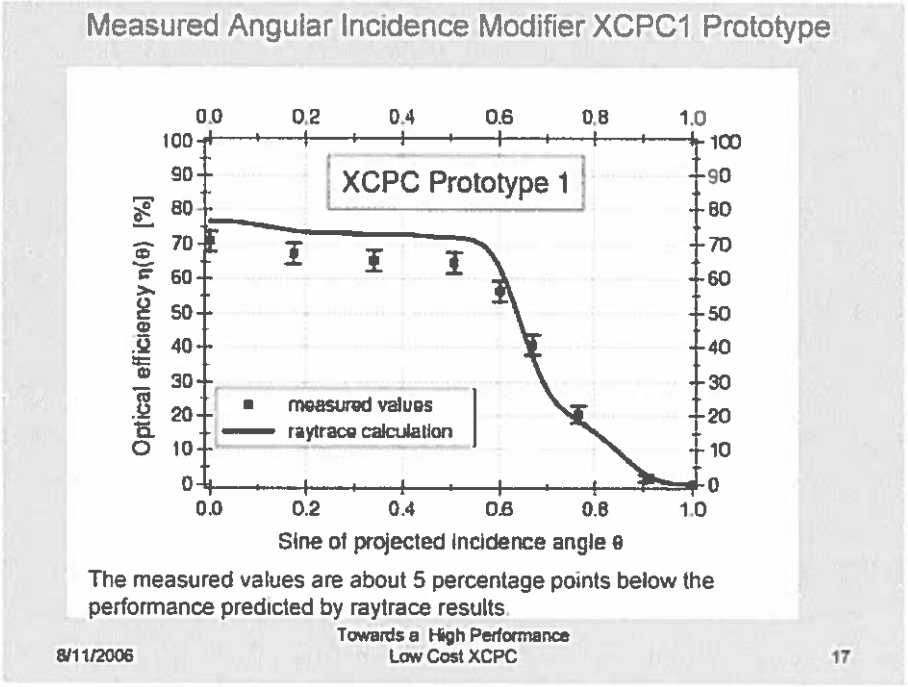

Solar Water Pumping System

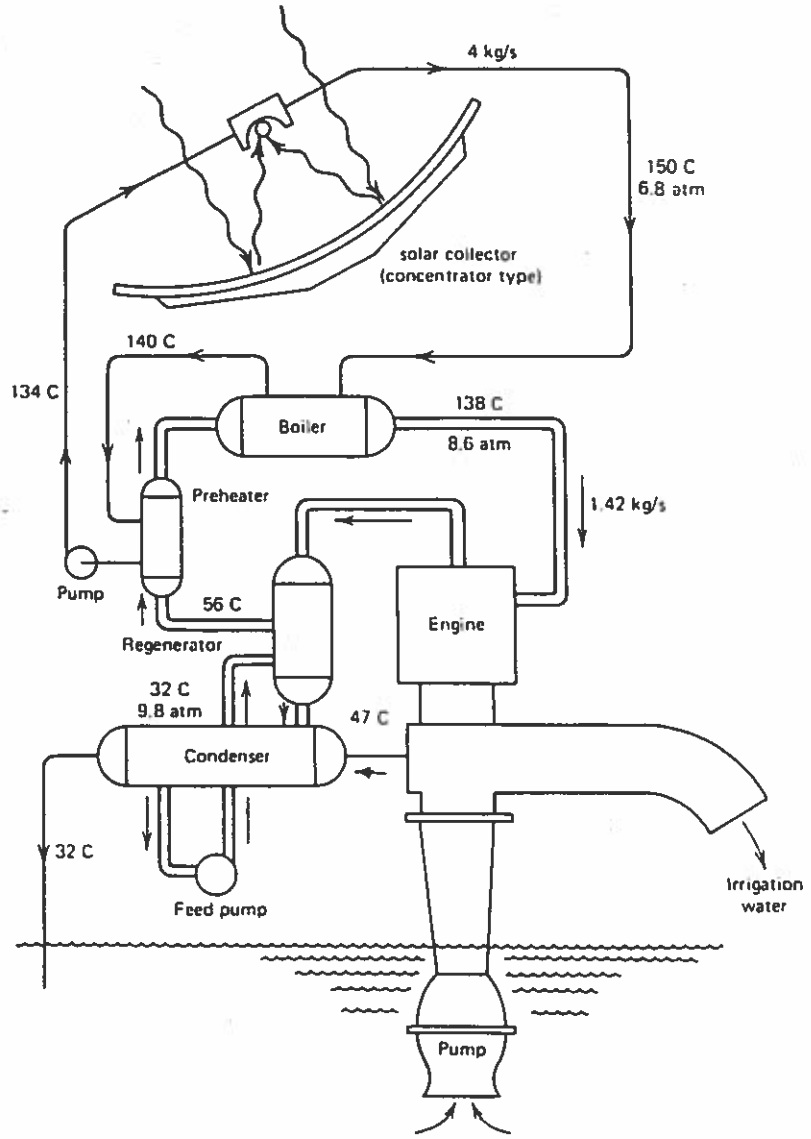

Figure 3-21 Solar powered water pumping station

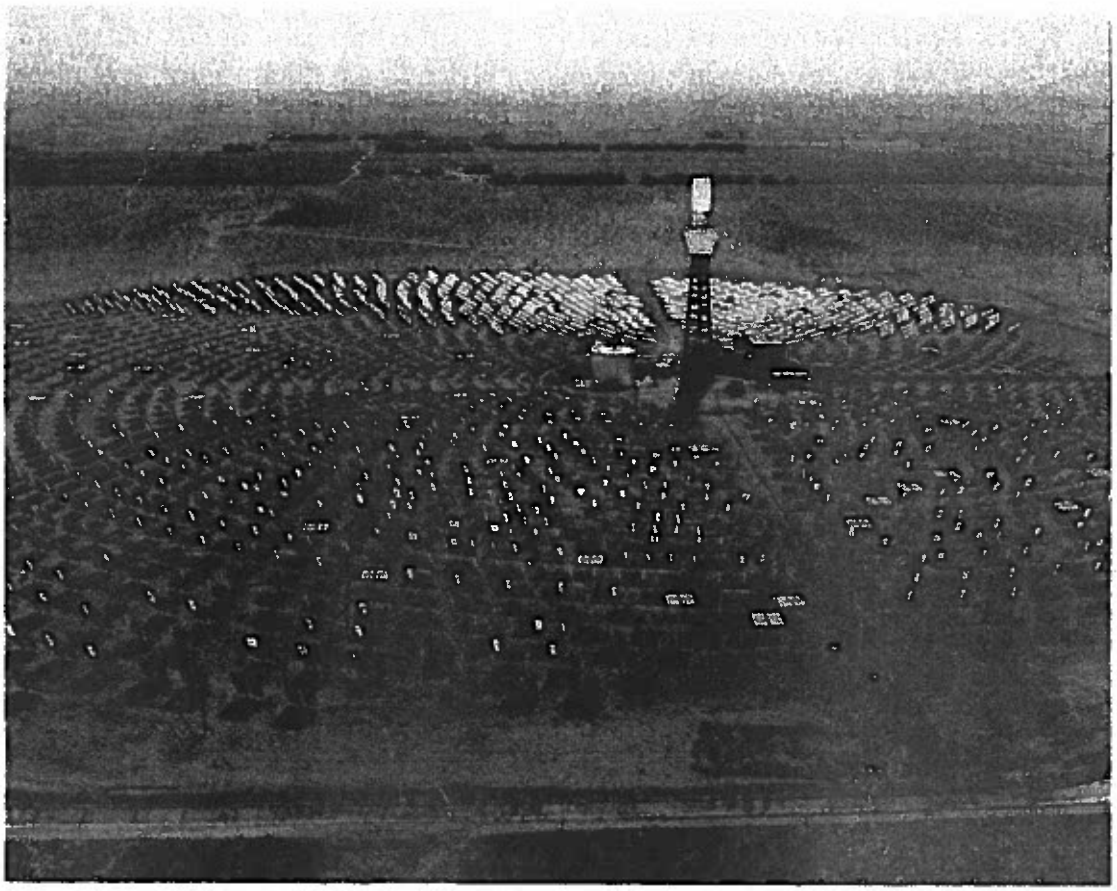

Figure 13-18 Overall view of Solar One, a 10-MW(e) (peak) central-receiver pilot powerplant near Barstow, California.

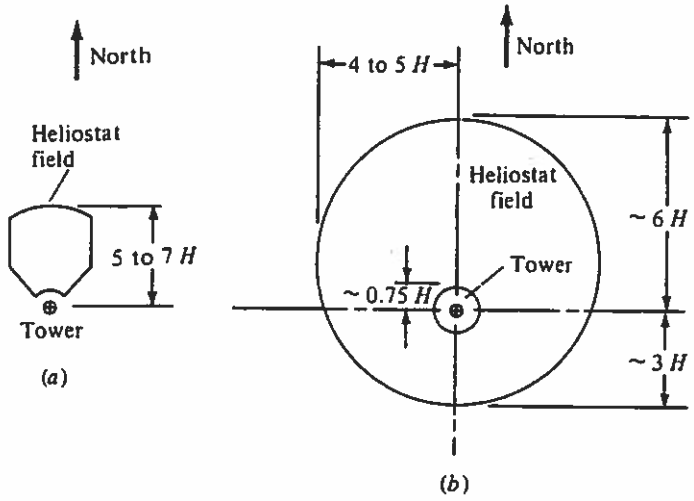

Figure 13-10 Optimum heliostat field shapes oriented for the northern hemisphere: (*a*) small plant < 100 MW(t) and (*b*) large plant > 5000 MW(t). Dimensions in multiples of receiver-tower height H [118].

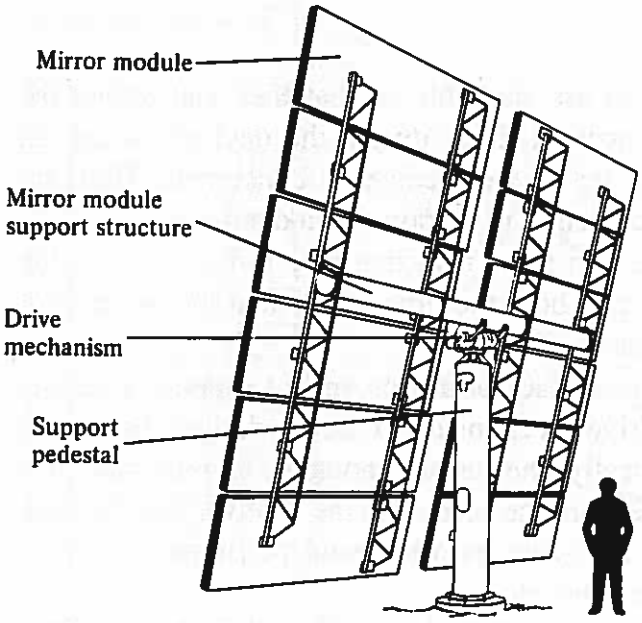

Figure 13-8 A typical glass-heliostat system, rear view *(McDonnell Douglas.)*

The Heliostat Field

The *heliostat field* supplying a central receiver, also called the *collector subsystem*, has a shape that must be optimized to suit the topography of the area and the power level of the plant. The field may be on a flat terrain, on the side of a hill, etc. In the northern hemisphere, the noontime sun is always south of the central-receiver tower, so a north field is usually most cost-effective because its cosine loss (below) is least.

For small plants, of less than 100 MW of thermal-energy input, a totally north field is optimum (Fig. 13-10*a*). As plant size increases, the field becomes larger and many heliostats are farther from the tower. The atmosphere around the plant attenuates the reflected radiation from the most distant north heliostats. The receiver input can then be improved by relocating the distant heliostats to the east and west of the tower and, as plant size increases further, to the south of it (Fig. 13-10*b*). In such cases, the additional cosine loss is less than the atmospheric attenuation loss from the distant north heliostats.

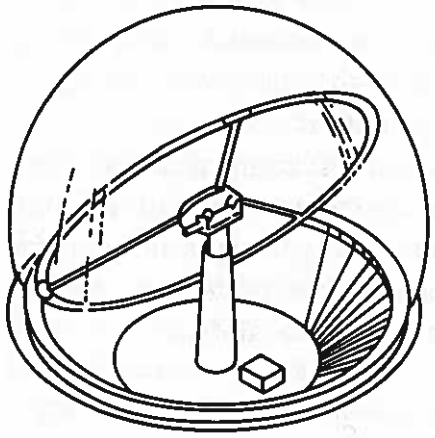

Figure 13-9 A typical plastic heliostat system *(Boeing.)*

SOLAR THERMAL ELECTRIC: CENTRAL RECEIVER

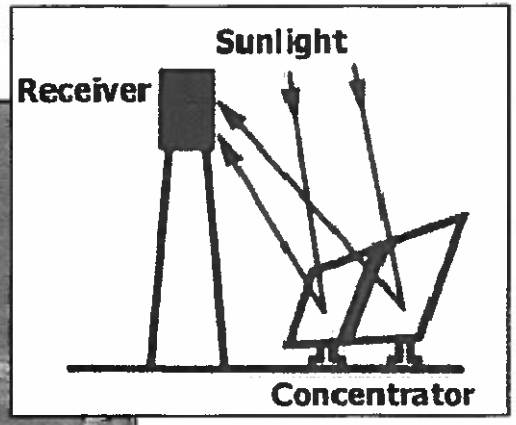

SOLAR THERMAL ELECTRIC: CENTRAL RECEIVER

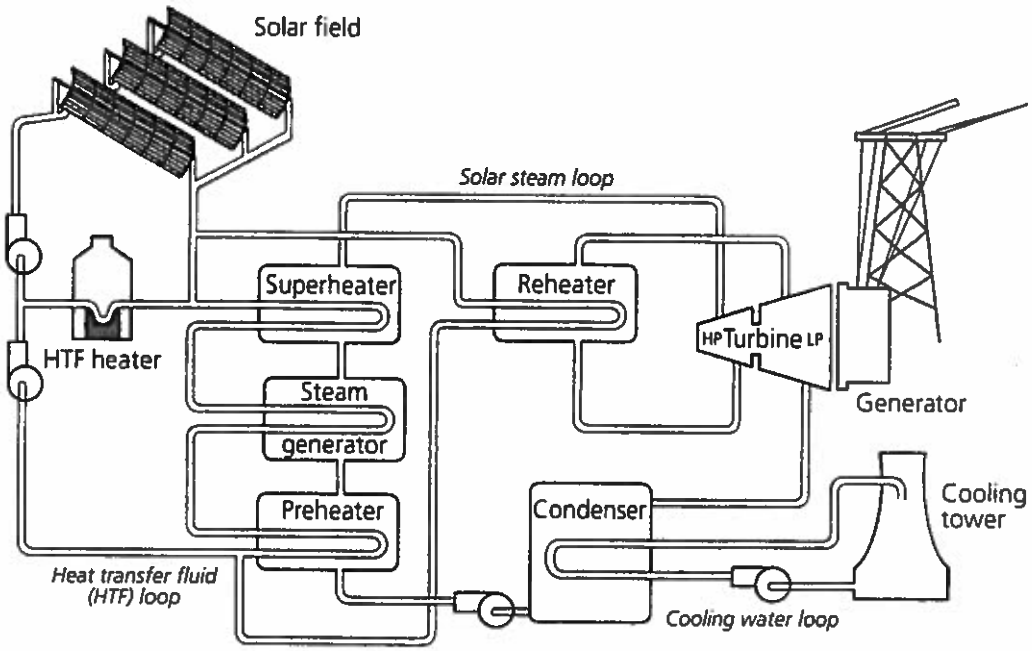

Figure 8.18. Flow of heat-transfer fluid through the SEGS VIII and IX plants (Adapted from [8]).

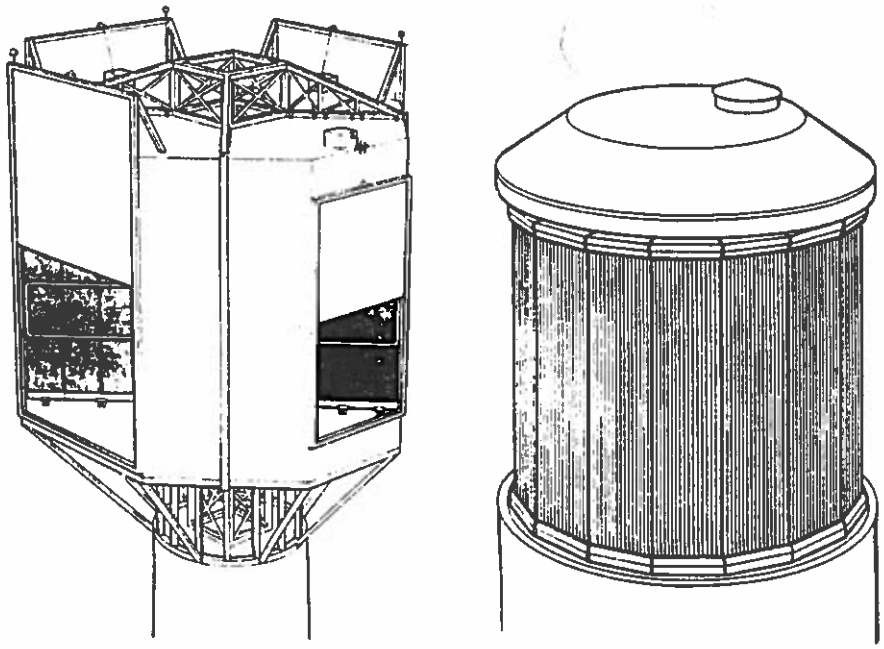

Figure 13-13 Typical central receivers: (*a*) four-aperture cavity type and (*b*) external type [118].

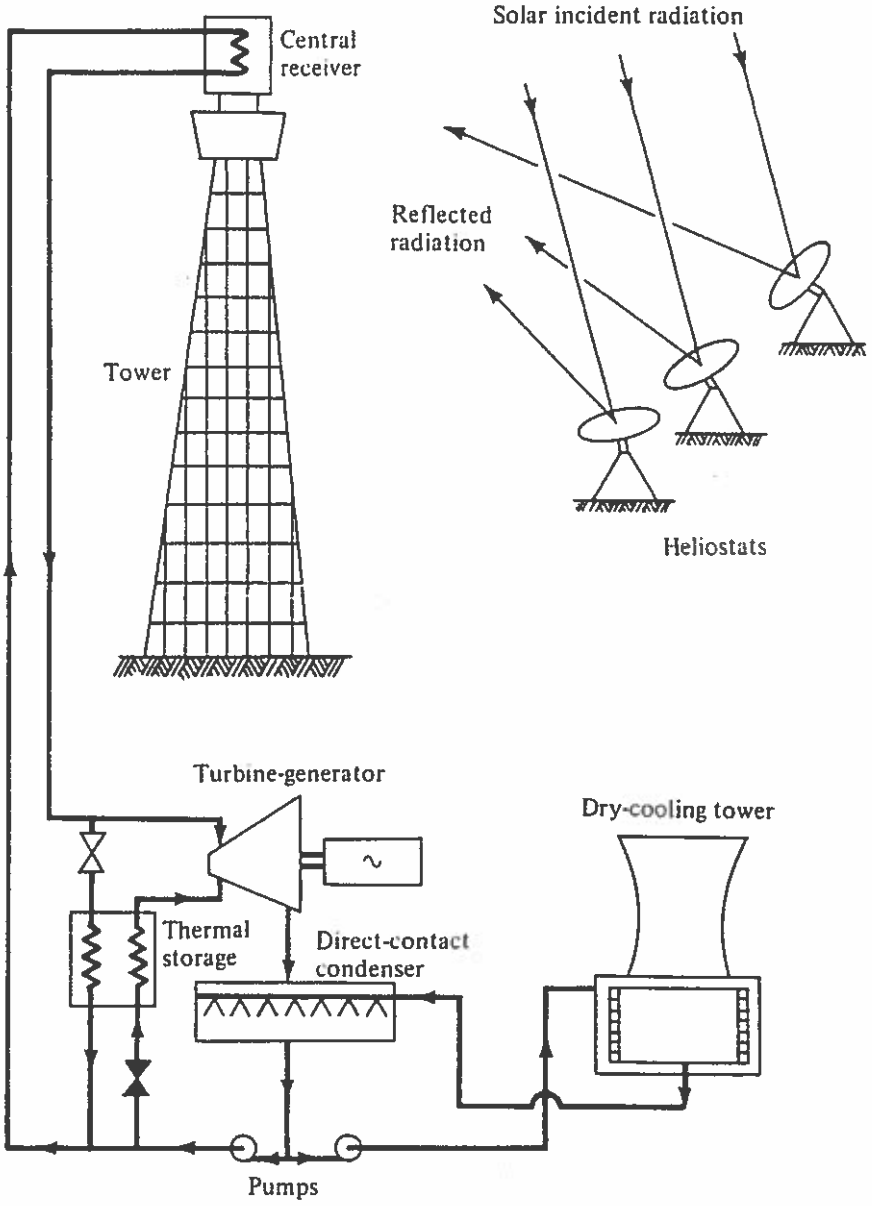

Figure 13-7 Schematic of a solar-thermal central-receiver system powerplant.

to the storage system, instead of to the receiver, where it vaporizes for use i turbine. Proper valving in the system allows operation in either mode.

Because solar-thermal electric plants are most likely to be located in hot arid where land is plentiful (for the large heliostat field) and where the sun's ener plentiful and dependable, but where cooling water is scarce, the condenser wa most probably cooled by a dry-cooling tower. Such towers are less effective and

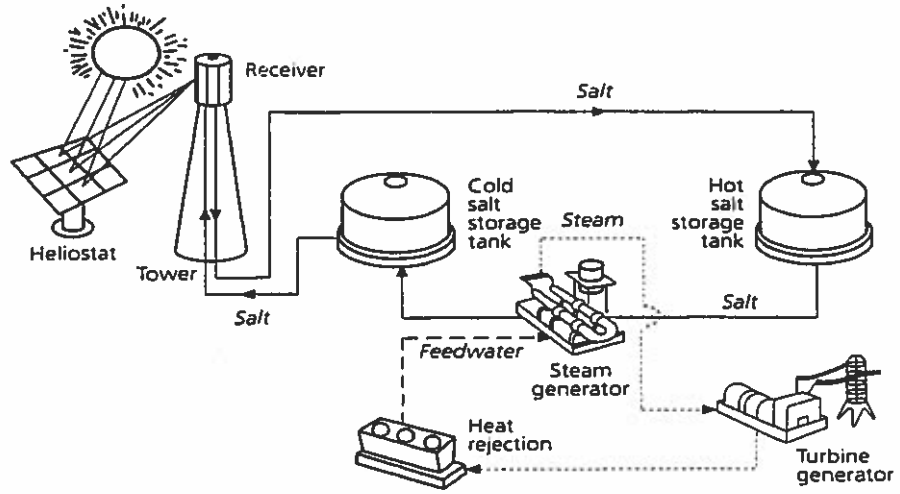

Figure 8.20. Schematic of Solar Two central-receiver plant configuration (Adapted from [8]).

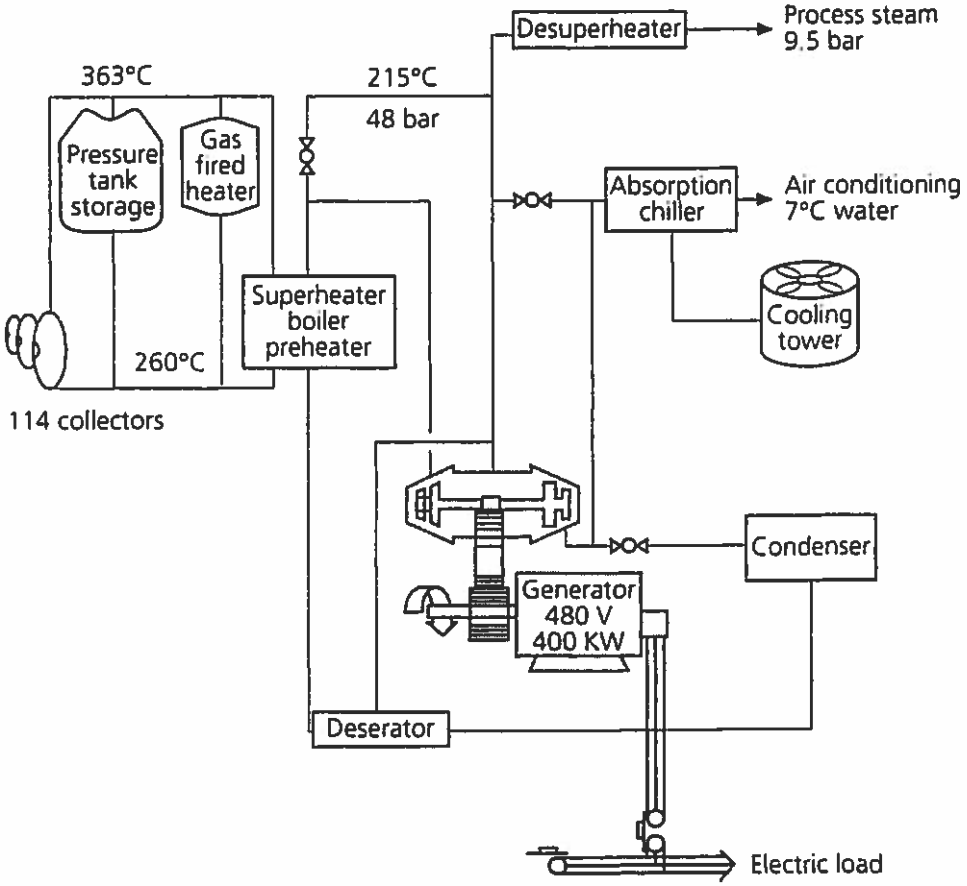

Figure 8.21. Schematic of the Shenandoah Solar Total Energy Project [8].

Table 3.1. Types of solar thermal collectors and their typical temperature range

Type of Collector	Concentration Ratio	Typical Working Temperature Range (°C)
Flat plate collector	1	≤70
High efficiency flat plate collector	1	60–120
Fixed concentrator	3–5	100–150
Parabolic trough collector	10–50	150–350
Parabolic dish collector	200–500	250–700
Central receiver	500–>3000	500–>1000

3.1 RADIATIVE PROPERTIES AND CHARACTERISTICS OF MATERIALS

When radiation strikes a body, a part of it is reflected, a part is absorbed and, if the material is transparent, a part is transmitted, as shown in Fig. 3.1.

The fraction of the incident radiation reflected is defined as the reflectance ρ, the fraction absorbed as the absorptance α, and the fraction transmitted as the transmittance τ. According to the first law of thermodynamics these three components must add up to unity, or

$$\alpha + \tau + \rho = 1. \tag{3.1}$$

Opaque bodies do not transmit any radiation and $\tau = 0$.

The reflection of radiation can be ***specular*** or ***diffuse***. When the angle of incidence is equal to the angle of reflection, the reflection is called specular; when the reflected radiation is uniformly distributed into all directions it is called diffuse (see Fig. 3.2). No real surface is either specular or diffuse, but a highly polished surface approaches specular reflection, whereas a rough surface reflects diffusely.